# Structural signatures of mobility on intermediate time scales in a supercooled fluid

William P. Krekelberg,[1] Venkat Ganesan,[1] and Thomas M. Truskett[1,2,*]

[1]*Department of Chemical Engineering, University of Texas at Austin, Austin, TX 78712.*
[2]*Institute for Theoretical Chemistry, University of Texas at Austin, Austin, TX 78712.*

We use simulation to explore how a particle's displacement in a supercooled fluid relates to its dynamic structural environment. The fluid we study, a binary mixture of hard spheres, exhibits classic signatures of dynamic heterogeneity, including a bimodal displacement distribution with distinct subpopulations of immobile and mobile particles on intermediate times. We find that immobile particles are readily distinguished from mobile particles by the overall strength of their pair correlations to their neighbors during the period of observation, but not simply by their average coordination number.

When fluids are supercooled (or overcompressed) toward their glass transition, their single-particle dynamics undergo qualitative changes.[1,2,3,4,5,6,7] One striking example is the distribution of particle displacements at intermediate time scales becomes bimodal, exhibiting distinct subpopulations of slow and fast particles.[2,6,7,8,9,10,11,12,13,14,15,16,17,18,19,20,21,22,23] This "heterogeneity" in dynamics has attracted interest because of its perceived consequences for other processes in deeply supercooled liquids including the breakdown of the Stokes-Einstein relationship[6,8,24,25,26] and the emergence of non-exponential trends in relaxation of the structure factor.[6,27]

Here we report results from a simulation based investigation of the following question about heterogeneous single-particle dynamics in supercooled liquids. "Is a particle's mean-square displacement over intermediate time scales closely related to the strength of its structural correlations to its neighbors during the displacement?" In other words, do fast particles experience a significantly more disordered structural environment (and slow particles a more ordered environment)? While the answer to this question may not establish a mechanism for the bimodal displacement distributions that occur near structural arrest, it will bring into focus the specific aspects of local structure (if any) that accompany, and perhaps facilitate, these pronounced dynamic characteristics. This, in turn, could help to strengthen our intuitive and theoretical understanding of related relaxation processes.

To address the issue posed above for a simple model, we study dense, binary fluid mixtures of hard spheres using event-driven molecular dynamics simulations.[28] We set the ratio of particle diameters in these mixtures to $\sigma_1/\sigma_2 = 1.3$ and the ratio of particle masses to $m_1/m_2 = (\sigma_1/\sigma_2)^3$, parameters that mimic concentrated colloidal suspensions that were recently investigated experimentally.[29] We simulate $N_1 = N_2 = 1000$ particles in a periodically-replicated cubic cell of volume $V$. We present results for particle packing fractions $\varphi = \pi(N_1\sigma_1^3 + N_2\sigma_2^3)/6V$ of 0.57 and 0.582, which, as we show below, correspond to state points with unimodal and bimodal displacement distributions on intermediate time scales, respectively. For brevity, we report quantities that are implicitly nondimensionalized by appropriate combinations of the length scale, $l_c = \sigma_2$ and time scale $t_c = \sqrt{m_2\sigma_2^2/k_B T}$, where $k_B$ is Boltzmann's constant. We focus on the dynamics and structure of the smaller type 2 particles, but we note that the behavior of the larger type 1 particles (not shown here) is qualitatively similar, as might be expected given the mild particle-size asymmetry of the fluid.

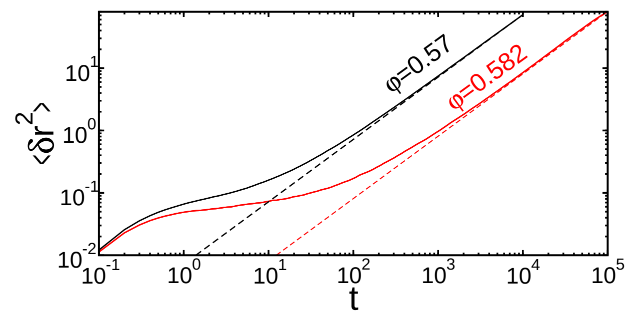


FIG. 1: (Color online) Mean-square displacement $\langle \delta r^2 \rangle$ of the smaller (type 2) particles versus time $t$ at packing fraction $\varphi = 0.57$ (black) and 0.582 (red). Dashed lines are fits of the Einstein relation $\langle \delta r^2 \rangle = 6Dt$ to the long-time behavior, resulting in tracer diffusion coefficients of $D = 1.2 \times 10^{-3}$ and $1.5 \times 10^{-4}$ at $\varphi = 0.57$ and 0.582, respectively.

We begin by examining the time $t$ dependence of the average mean-square displacement, $\langle \delta r^2 \rangle$, for the type 2 particles. In particular, Figure 1 displays results for packing fractions of $\varphi = 0.57$ and 0.582. At both state points, the fluid exhibits a mean-square displacement plateau at intermediate times, which is characteristic of "cage" dynamics.[30] Schematically, the plateau separates the ballistic motion that occurs at very short times (before motion is temporarily hindered by collisions with the cage of nearest-neighbor particles) and the diffusive motion that particles ultimately attain at long times (after breaking through the cage). As should be expected, the plateau occurs at smaller displacements and persists for longer times when $\varphi$ is increased, indicating that the cage formed by the nearest-neighbor coordination shell becomes both tighter and more difficult to disrupt at higher packing fraction.

In order to characterize dynamic heterogeneities of the type 2 particles at the state points examined above, we

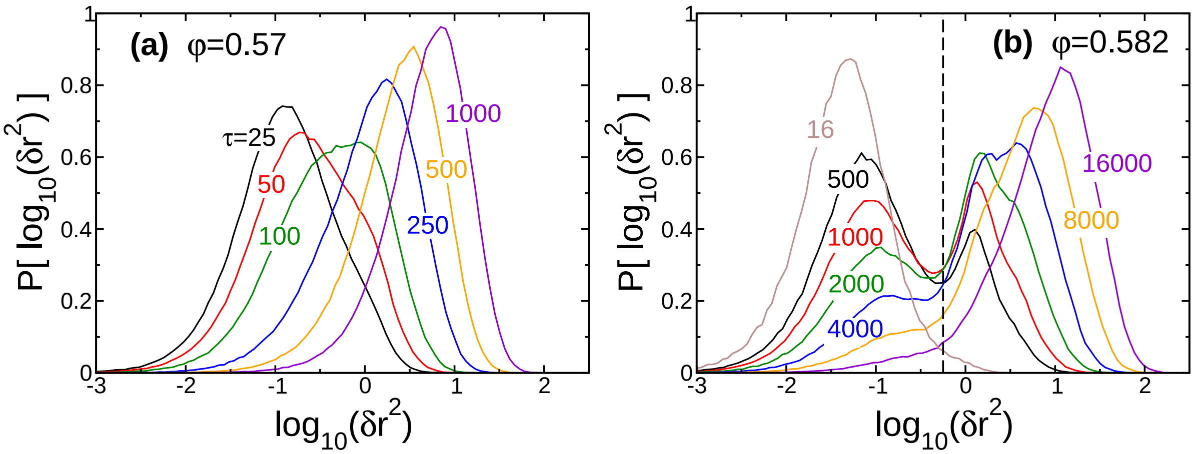


FIG. 2: (Color online) Distribution of the logarithm of mean-square displacement $P[\log_{10}(\delta r^2)]$ for type 2 particles of the binary hard-sphere mixture described in the text. Data cover several time intervals $t = \tau$ for packing fractions **(a)** $\varphi = 0.57$ and **(b)** $\varphi = 0.582$. The numbers in the figure provide the value of $\tau$ for each curve. In **(b)**, the vertical line is at $\delta r^2 = 0.56$, the approximate dividing line between mobile and immobile particles discussed in the text.

follow Ref. 31 and investigate the distributions of the logarithm of the mean-square displacement ($P[\log_{10}(\delta r^2)]$) over a variety of time intervals ($t = \tau$). Specifically, Figure 2a displays $P[\log_{10}(\delta r^2)]$ for the fluid at $\varphi = 0.57$ and values of $\tau$ that correspond to average mean-square displacements which span from the plateau "cage" region to the beginning of the diffusive regime (see Figure 1). The main point of Figure 2a is that, for all values of $\tau$, $P[\log_{10}(\delta r^2)]$ remains unimodal, indicating that pronounced single-particle dynamic heterogeneities have not yet emerged in the fluid at this packing fraction. However, also notice that for the displacement distributions corresponding to intermediate times, particularly at $\tau = 50$, a shoulder at higher mean-square displacements becomes evident. This shoulder is a precursor to the bimodal displacement behavior that occurs at $\varphi = 0.582$, which we discuss in detail below.

Figure 2b displays the behavior of $P[\log_{10}(\delta r^2)]$ at $\varphi = 0.582$. Notice that, for intermediate times before diffusive behavior is reached ($500 \leq \tau \leq 4000$), $P[\log_{10}(\delta r^2)]$ is unambiguously bimodal. That is, there are clear subpopulations of slower and faster particles. A boundary between the two subpopulations can be drawn at $\delta r^2 \approx 0.56$ (vertical dashed line in Figure 1), which distinguishes the particles that are still caged on intermediate time scales from those that have broken through their nearest-neighbor coordination shells to attain larger displacements. For descriptive purposes, we label particles with $\delta r^2 < 0.56$ "immobile" (on these time scales), while we label those with $\delta r^2 > 0.56$ "mobile". The type of dynamic behavior depicted in Figure 2b has been well documented in other systems.[32] Below, we investigate whether the immobile particles experience, on average, a more structurally ordered environment than the mobile particles during the time intervals of their respective displacements.

To carry out the analysis described above, we first examine our simulation trajectories to accumulate statistics for each time interval $\tau$, classifying type 2 particles according to the logarithm of their mean-square displacement during the observation period. This amounts to creating a histogram from the distributions shown in Figures 2a and 2b, assigning type 2 particles to "mobility bins". Depending on the value of $\tau$, we use bin sizes in the range 0.1 - 0.2 $\log_{10}(\delta r^2)$, which we find is sufficiently narrow to capture the shapes of the mobility distributions, but coarse enough to allow for excellent statistical sampling. We then compute the pair correlation function, $\widetilde{g}_{2j}(r)$, between the type 2 particles in a particular $\tau$-dependent mobility bin and *all* surrounding particles of type $j$. In this work, the $\sim$ overbar denotes a quantity that describes the structure surrounding certain type 2 particles, i.e., those which populate a specific mobility bin for time interval $\tau$.[33]

In order to convert the structural information contained in the $\widetilde{g}_{2j}(r)$ into a number that characterizes the degree of pair translational order that a type 2 particle (in given a mobility bin) experiences during the course of its displacement, we compute $-\widetilde{s}_2$, which we define as

$$-\widetilde{s}_2 \equiv \frac{\rho}{2}\sum_j x_j \int_0^\infty d\mathbf{r}\{\widetilde{g}_{2j}(\mathbf{r})\ln\,\widetilde{g}_{2j}(\mathbf{r}) - [\widetilde{g}_{2j}(\mathbf{r}) - 1]\}. \tag{1}$$

Here, $\rho = (N_1 + N_2)/V$ is the total number density, and $x_j$ is the mole fraction of component $j$. This measure is a dynamic generalization of a static structural metric, $-s_2^{(2)}$, which quantifies the contribution to the excess entropy of a mixture arising from equilibrium pair correlations involving particles of type 2. In fact, our motivation for using $-\widetilde{s}_2$ in this study comes from (1) the earlier empirical observation[34,35] that the long-time tracer diffusivity of species $i$ in equilibrium mixtures scales in a simple way with the static measure $-s_2^{(2)}$ and (2) the wider literature demonstrating that excess entropy captures many of the effects that temperature, density, and confinement have on the transport coefficients of equilibrium fluids (see, e.g., Refs. 36,37,38,39). Although we focus exclusively on the quantity $-\widetilde{s}_2$ in this paper to characterize structure, we have found that other commonly used structural order metrics[40] calculable from $\widetilde{g}_{2j}(r)$ produce qualitatively similar results.

Now we examine the connection between displacement and structural order for type 2 particles in the system at $\varphi = 0.57$, a supercooled fluid state point for which pronounced dynamic heterogeneities have not yet emerged. Figure 3a shows that there is a clear negative correlation between the local structural order $-\widetilde{s}_2$ surrounding a particle during an observation window $\tau$ and how far it moves in that time frame. As one might expect, the slope of this correlation depends of the value of $\tau$. Larger vibrational displacements in short time frames (small $\tau$) appear to require a significant amount of local disorder (e.g., distortion of the cage of first neighbors), whereas less structural disorder over the course of the displacement appears necessary for significant particle motion on longer time scales (i.e., the diffusive limit). The transition from short to longer time behavior appears smooth at this packing fraction.

The behavior is different, however, for the fluid at $\varphi = 0.582$ where the bimodal displacement distribution characteristic of strong dynamic heterogeneities is observed (see Figure 3b). In particular, there is now a sharp change in the slope of the correlation between structure and dynamics when one compares "immobile" versus "mobile" particles. For immobile caged particles, one again finds a strong negative correlation between the local structure and particle displacement, indicating that larger vibrational displacements generally require significant cage distortion. For mobile particles, however, the relation between structural order and mobility is nearly flat. This flatness indicates that while not all structural disorder leads to high mobility, a critical amount of maintained structural disorder (i.e., cage breaking), appears necessary for larger displacements to occur on a given time frame. We can characterize the amount of structural order that needs to be maintained by the cage to localize particles on time scale $\tau$ as $-\widetilde{s}_{2,\mathrm{C}} \equiv -\widetilde{s}_2(\delta r^2 = 0.56)$. As shown in the inset to Fig. 3b, $-\widetilde{s}_{2,\mathrm{C}}$ increases logarithmically with $\tau$ under these conditions.

If we focus on the structure and dynamics of mobile particles, a minor secondary effect in Figure 3b is also worth noting. Specifically, those particles with intermediate displacements (of the order of a single particle diameter) on a time scale $\tau$ can have slightly more structural order than those with either smaller or larger displacements. This small effect is perhaps expected and likely due to recaging events, where a new coordination shell is temporarily formed around a particle that has travelled just far enough to "break free" from its original set of nearest neighbors.

Given the above results, one might logically ask whether a simple measure like coordination number, which roughly characterizes local density surrounding a particle, might provide the same qualitative information as $-\widetilde{s}_2$. To test this idea, we have also collected statistics on $\widetilde{n}_{\mathrm{tot}} \equiv 4\pi \sum_j x_j \rho \int_0^{r_{\mathrm{min},j}} r^2 \widetilde{g}_{2j}(r) dr$, the average number of nearest neighbors surrounding type 2 particles (in a given mobility bin on time interval $\tau$). Here, $r_{\mathrm{min},j}$ is the location of the first minimum in $\widetilde{g}_{2j}(r)$.

Figures 4a and b display $\widetilde{n}_{\mathrm{tot}}$ as a function of $\log_{10}(\delta r^2)$ for $\varphi = 0.57$ and 0.582, respectively. Note that, in contrast to $-\widetilde{s}_2$, the coordination number does not provide a clear indication of the different structural environments that surround mobile versus immobile particles on intermediate time scales. This suggests that consideration of average positional correlations beyond the first neighbor shell are key to understanding how the local (dynamic) structure correlates to, and perhaps facilitates, single-particle mobility in deeply supercooled fluids.

Two authors (T.M.T. and V.G.) acknowledge support of the Welch Foundation (F-1696 and F-1599, respectively). One author (T.M.T) acknowledges financial support of the National Science Foundation (CTS-0448721) and the David and Lucile Packard Foundation. The Texas Advanced Computing Center (TACC) provided computational resources for this study.

---

* Electronic address: truskett@che.utexas.edu; Corresponding Author


1 D. N. Perera and P. Harrowell, Phys. Rev. E **54**, 1652 (1996).

2 W. Kob, C. Donati, S. J. Plimpton, P. H. Poole, and S. C. Glotzer, Phys. Rev. Lett. **79**, 2827 (1997).

3 C. Donati, J. F. Douglas, W. Kob, S. J. Plimpton, P. H. Poole, and S. C. Glotzer, Phys. Rev. Lett. **80**, 2338 (1998).

4 R. Yamamoto and A. Onuki, Phys. Rev. E **58**, 3515 (1998).

5 C. A. Angell, K. L. Ngai, G. B. McKenna, P. F. McMillan, and S. W. Martin, J. Appl. Phys. **88**, 3113 (2000).

6 M. D. Ediger, Annu. Rev. Phys. Chem. **51**, 99 (2000).

7 K. S. Schweizer, Curr. Opin. Colloid In. **12**, 297 (2007).

8 R. Yamamoto and A. Onuki, Phys. Rev. Lett. **81**, 4915 (1998).

9 S. C. Glotzer and C. Donati, J. Phys.: Condens. Matter **11**, A285 (1999).

10 E. Vidal Russell and N. E. Israeloff, Nature **408**, 695 (2000).

11 S. C. Glotzer, V. N. Novikov, and T. B. Schrøder, J. Chem. Phys. **112**, 509 (2000).

12 S. C. Glotzer, J. Non-Cryst. Solids **274**, 342 (2000).

13 E. R. Weeks, J. C. Crocker, A. C. Levitt, A. Schofield, and D. A. Weitz, Science **287**, 627 (2000).

14 Y. Gebremichael, T. B. Schrøder, F. W. Starr, and S. C. Glotzer, Phys. Rev. E **64**, 051503 (2001).

15 S. A. Reinsberg, X. H. Qiu, M. Wilhelm, H. W. Spiess, and M. D. Ediger, J. Chem. Phys. **114**, 7299 (2001).

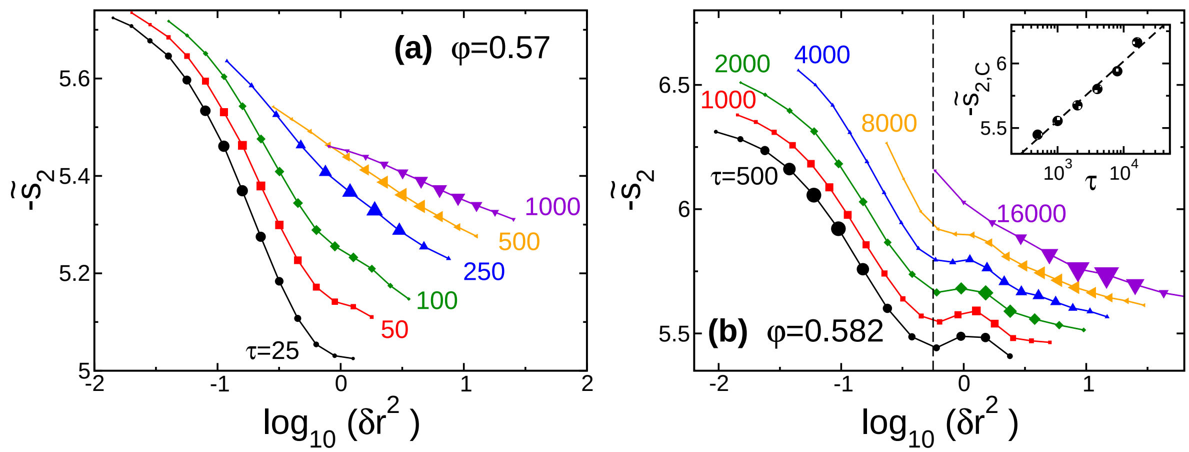


FIG. 3: (Color online) Average structural order metric $-\widetilde{s}_2$ that type 2 particles of the binary mixture discussed in the text experience during an observation time $\tau$ as a function of the logarithm of their mean-square displacement $\log_{10}(\delta r^2)$. Data is for packing fractions **(a)** $\varphi = 0.57$ and **(b)** $\varphi = 0.582$. The numbers in the figure correspond to the value of $\tau$ for the curve of the same color. The size of the symbol is proportional to the fraction of particles in the "mobility bin" centered at that value of $\log_{10}(\delta r^2)$. In **(b)**, the horizontal dashed line at $\delta r^2 = 0.56$ represents the boundary between mobile and immobile particles (see Figure 2b and text). The inset to **(b)** displays the value of $\widetilde{s}_2$ for $\delta r^2 = 0.56$, $\widetilde{s}_{2,\mathrm{C}} = \widetilde{s}_2(\delta r^2 = 0.56)$, as a function $\tau$.

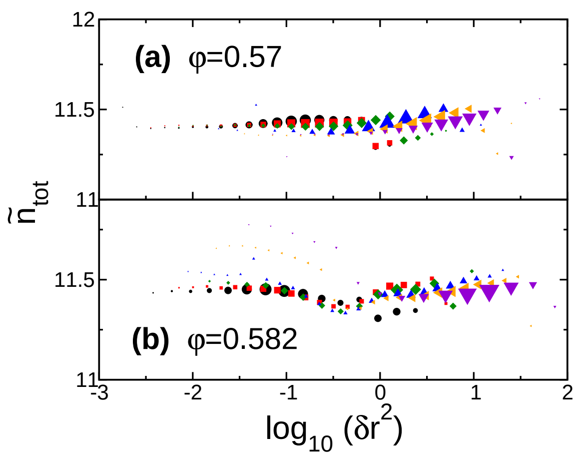


FIG. 4: (Color online) Average number of nearest neighbors, $\widetilde{n}_{\mathrm{tot}}$, for type 2 particles of the binary mixture discussed in the text during an observation time $\tau$ as a function of the logarithm of their mean-square displacement $\log_{10}(\delta r^2)$. Data is for packing fractions **(a)** $\varphi = 0.57$ and **(b)** $\varphi = 0.582$. The symbols are the same as those in Figure 3. The size of the symbols is proportional to the fraction of particles belonging to each mobility bin over time interval $\tau$.


[16] N. Lačević, F. W. Starr, T. B. Schrøder, and S. C. Glotzer, J. Chem. Phys. **119**, 7372 (2003).
[17] M. Vogel and S. C. Glotzer, Phys. Rev. E **70**, 061504 (2004).
[18] M. Vogel and S. C. Glotzer, Phys. Rev. Lett. **92**, 255901 (2004).
[19] A. M. Puertas, M. Fuchs, and M. E. Cates, cond-mat **1**, 0510443 (2005).
[20] D. R. Reichman, E. Rabani, and P. L. Geissler, J. Phys. Chem. B **109**, 14654 (2005).
[21] E. J. Saltzman and K. S. Schweizer, Physical Review E **74**, 061501 (2006).
[22] T. Kawasaki, T. Araki, and H. Tanaka, Phys. Rev. Lett. **99**, 215701 (2007).
[23] E. J. Saltzman and K. S. Schweizer, Phys. Rev. E **77**, 051504 (2008).
[24] F. H. Stillinger and J. A. Hodgdon, Phys. Rev. E **50**, 2064 (1994).
[25] G. Tarjus and D. Kivelson, J. Chem. Phys. **103**, 3071 (1995).
[26] S. K. Kumar, G. Szamel, and J. F. Douglas, J. Chem. Phys. **124**, 214501 (2006).
[27] B. Doliwa and A. Heuer, J. Phys.: Condens. Matter **11**, A277 (1999).
[28] D. C. Rapaport, *The Art of Molecular Dynamic Simulation* (Cambridge University Press, Cambridge, 2004), 2nd ed.
[29] C. R. Nugent, K. V. Edmond, H. N. Patel, and E. R. Weeks, Phys. Rev. Lett. **99**, 025702 (2007).
[30] E. R. Weeks and D. A. Weitz, Phys. Rev. Lett. **89**, 095704 (2002).
[31] M. E. Cates, M. Fuchs, K. Kroy, W. C. K. Poon, and A. M. Puertas, J. Phys.: Condens. Matter **16**, S4861 (2004).
[32] C. Donati, S. C. Glotzer, P. H. Poole, W. Kob, and S. J. Plimpton, Phys. Rev. E **60**, 3107 (1999).
[33] R. Palomar and G. Sesé, J. Chem. Phys. **129**, 064505 (2008).
[34] A. Samanta, S. M. Ali, and S. K. Ghosh, Phys. Rev. Lett. **87**, 245901 (2001).
[35] M. J. Pond, W. P. Krekelberg, V. K. Shen, J. R. Errington, and T. M. Truskett, J. Chem. Phys. **131**, 161101 (2009).
[36] M. Dzugutov, Nature **381**, 137 (1996).
[37] Y. Rosenfeld, J. Phys.: Condens. Matter **11**, 5415 (1999).
[38] G. Goel, W. P. Krekelberg, M. J. Pond, J. Mittal, V. K. Shen, J. R. Errington, and T. M. Truskett, J. Stat. Mech. **2009**, P04006 (2009).
[39] J. Mittal, J. R. Errington, and T. M. Truskett, Phys. Rev. Lett. **96**, 177804 (2006).
[40] T. M. Truskett, S. Torquato, and P. G. Debenedetti, Phys. Rev. E **62**, 993 (2000).